Son *et al. Micro and Nano Systems Letters* (2024) 12:4
https://doi.org/10.1186/s40486-023-00197-4

Micro and Nano Systems Letters

LETTER

Open Access

Study on repetitive damage-recovery cycle of hydrophobic coating for electrowetting-on-dielectric (EWOD) applications

Youngdoo Son[1], Woochan Kim[1], Daeyoung Lee[1*] and Sang Kug Chung[1*]

Abstract

This study is focusing on the durability of fluoropolymer hydrophobic coatings against falling droplets. Devices such as smart self-cleaning lens or droplet-based energy generators are open-air electrowetting-on-dielectric (EWOD) devices, which are applications that utilize falling droplets. Therefore, the hydrophobic coatings of these devices are exposed to environment factors such as raindrop, and it is necessary to examine the durability of hydrophobic coatings in similar environments and the effectiveness of recovery. Thus, in this study, we simulate raindrops to damage samples with various thicknesses of Cytop (CTX-809SP2). Subsequently, damaged samples are heated to recover their hydrophobicity, and we repeat this damage-recovery cycle several times to evaluate the long-term durability of hydrophobic coating. The EWOD samples of three different hydrophobic coating thicknesses (0.1 μm, 0.5 μm, and 1.0 μm) are damaged by falling droplets from a certain height for 10 days. The damaged samples are then recovered by heating them on a hot plate at 200 ℃ for 24 h and evaluate their EWOD performance. In addition, the hydrophobic coatings are repeatedly damaged and recovered several times to examine the number of recovery limitations of the coatings. After the second damage-recovery cycle, the thickest hydrophobic coating sample shows 7 % better EWOD performance than others. Additionally, after the third damage-recovery cycle, the EWOD performance of all samples significantly degrade, experimentally verifying the number of recovery limitations of the hydrophobic coating. The results of this study are expected to provide useful information for open-air EWOD devices on the methods for evaluating their durability and the thickness selection of hydrophobic coating.

Keywords Falling droplets, Contact angle, Contact angle hysteresis, Heat-treated, Fluoropolymer hydrophobic coating

Introduction

Water-repellent and hydrophobic coatings are increasingly common in daily life. Hydrophobic surfaces, which are also found in nature, play an important role in research and industry, and are applied in a variety of applications such as clothing, automobiles and window glasses etc [1]. Among them, the surface of the fluoropolymer hydrophobic coatings increases the contact angle of water droplets and makes them easy to roll off from the surface due to their low surface energy and low friction, respectively [2, 3]. In particular, a fluoropolymer

*Correspondence:
Daeyoung Lee
dylee@mju.ac.kr
Sang Kug Chung
skchung@mju.ac.kr
[1] Department of Mechanical Engineering, Myongji University, Yong-in 17058, Republic of Korea

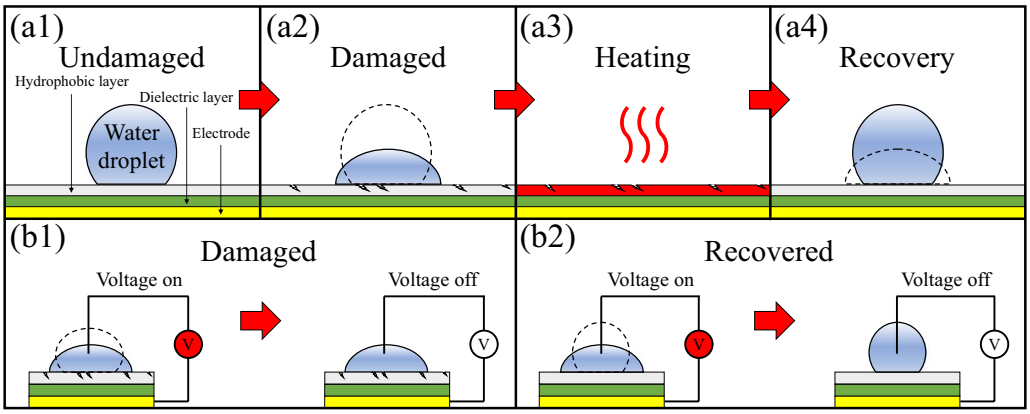

Fig. 1 Schematic diagram of **a** damage-recovery cycle of hydrophobic coating; **b** changes in electrowetting-on-dielectric (EWOD) performance due to damage and recovery of hydrophobic coating

hydrophobic coating called Cytop is commonly used in electrowetting-on-dielectric (EWOD) technology because of these properties. EWOD technology has recently gained attention in the Micro Electro Mechanical Systems (MEMS) application due to its fast response time and low power consumption among the droplet control technologies [4] such as surface acoustic wave (SAW) [5, 6], mechanical drive [7, 8], and thermal capillary [9–11]. For these reasons, a variety of applications using EWOD technology, such as lab-on-a-chip [12–14], liquid lens [15–19], liquid shutter [20], electrowetting display (EWD) [21–23], smart self-cleaning lens [24], and droplet-based energy generator [25–29] have been developed.

However, it has been noted that the hydrophobic coating, which plays a crucial role in EWOD devices, degrades its hydrophobicity due to prolonged water exposure and repeated EWOD actuations, etc [2, 3, 30–32]. To overcome these limitations, research has been conducted to recover damaged hydrophobic coatings. Zeng et al. conducted a study on recovering the Teflon AF hydrophobic coatings applied to EWOD-based chemiluminescence detectors. Teflon AF damaged by the chemiluminescence reaction was heated at various temperatures to quantify the recovery characteristics of the coating as a function of time and temperature [32]. Trapuzzano et al. damaged a variety of fluoropolymer coatings commonly used in the EWOD industry through long-term water exposure, and then demonstrated that certain coatings could recover their hydrophobicity by heating [2]. However, these studies focused on the damage and recovery methods of the hydrophobic coating and did not provide information on the long-term durability of the coating. In addition, open-air EWOD devices such as smart self-cleaning lens [24] and droplet-based energy generator [25–29] require consideration of damage variables that differ from water immersion. Therefore, this study evaluates the durability of open-air EWOD devices by simulating raindrop damage to hydrophobic coatings and comparing the durability of different hydrophobic coating thicknesses.

Figure 1 is the concept of this study. The Cytop (CTX-809SP2) hydrophobic coatings with different thicknesses are damaged by a raindrop simulation. (Fig. 1a1-2) The

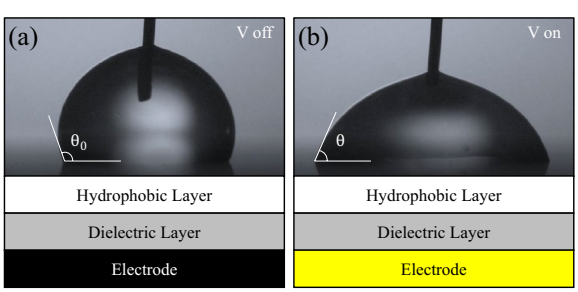

Fig. 2 Wettability changes in EWOD: **a** initial state and **b** after voltage is applied between a conducting droplet and an electrode

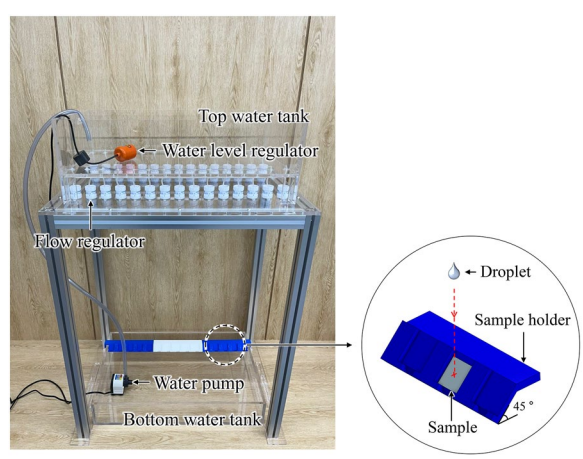

Fig. 3 Experimental setup for simulating raindrops

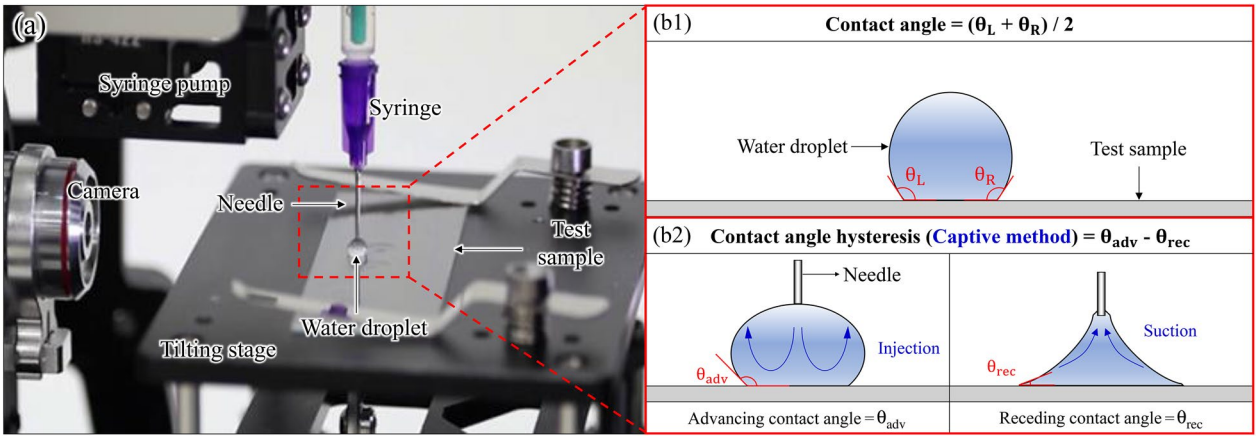

Fig. 4 Measurement of contact angle and contact angle hysteresis by a contact angle goniometer (Smartdrop, Femtobiomed Inc.)

damaged hydrophobic coatings are then heated on a 200 ℃ hot plate for 24 h to recover their hydrophobicity (Fig. 1a3-4) [33]. This process of heating and recovering damaged hydrophobic coatings is called the damage-recovery cycle (Fig. 1a1-4). In a previous study, the contact angle (CA) and contact angle hysteresis (CAH) of droplets placed on the hydrophobic coating were evaluated to determine the recovery of the hydrophobic coating by heating [2]. In this study, we not only evaluate the CA and CAH of droplets placed on the hydrophobic coating but also analyze the performance of EWOD actuation to verify the recovery of the hydrophobic coating (Fig. 1b). This allows to analyze the trend of damage and recovery as a function of the thickness of the hydrophobic

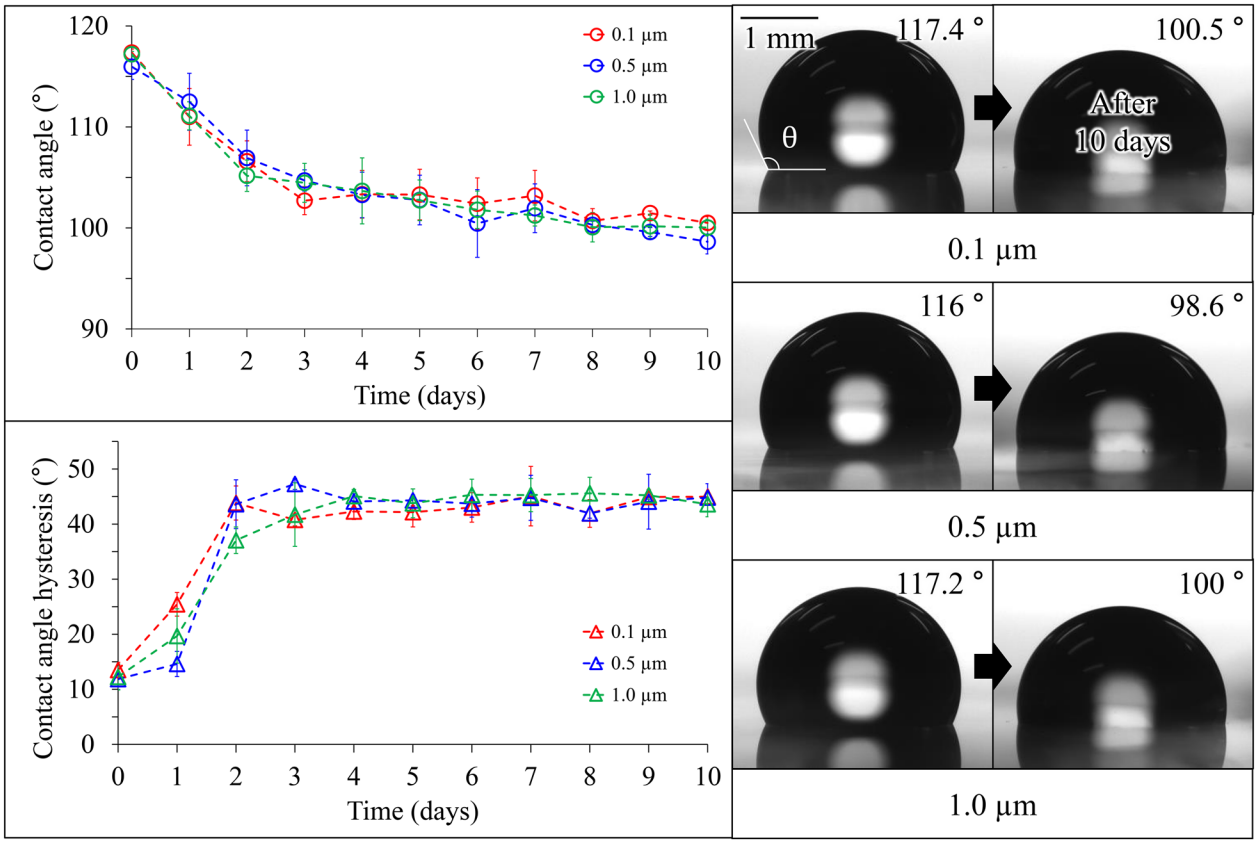

Fig. 5 Graph of the change in contact angle and contact angle hysteresis for the samples damaged by falling droplets over 10 days

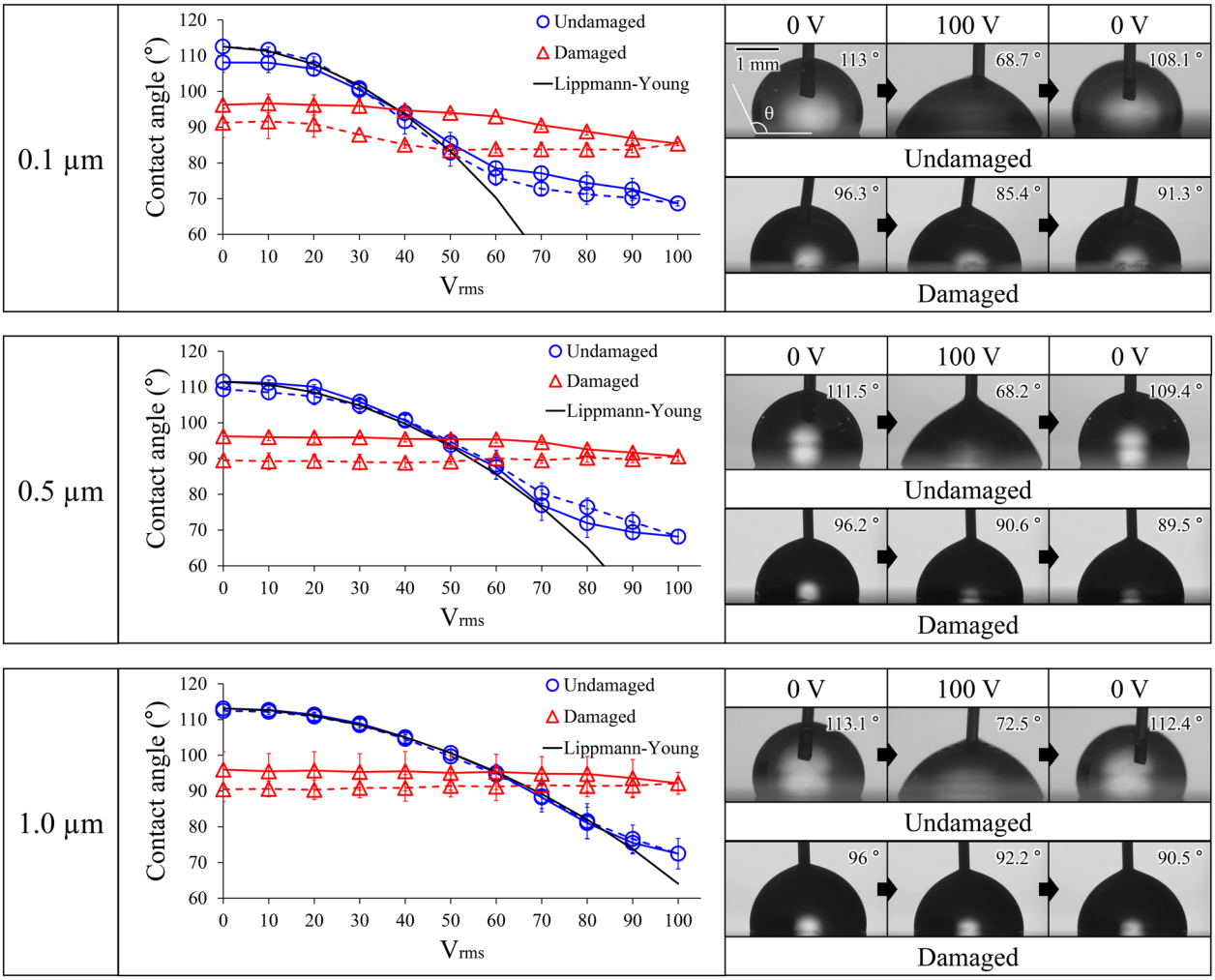

Fig. 6 EWOD hysteresis graph of the damaged samples and the undamaged samples; the solid line is for increasing voltage, and the dashed line is for decreasing voltage

coating, and to verify the number of recovery limitations of the hydrophobic coating by repeating the damage-recovery cycle. Therefore, this study is expected to provide useful information on how to evaluate the durability of hydrophobic coatings in open-air EWOD devices and the selection of their thickness (Fig. 2).

Theoretical background

The theoretical basis of EWOD was established in the early 2000s [34]. The relationship between voltage and CA, which is given by the so-called Lippmann-Young equation, theoretically describes the physical phenomenon of EWOD. Upon applying a voltage between a conductive droplet and a dielectric layer-coated electrode, an electric double layer builds up near the solid–liquid interfaces in the dielectric layer spontaneously [35, 36]. Since the accumulation of the opposite charges around the three-phase contact line (TCL) near the solid surface, reduction of the interfacial tension causes the droplet to spread out under the applied electric field, as shown in Fig. 2 [35]. Berge et al. substituted the Lippmann equation, which describes the relationship between applied voltage and droplet contact angle into the Young's equation, which describes the relationship between interface and droplet contact angle, and derived the following equation [37]:

$$\cos\theta = \cos\theta_0 + \frac{\varepsilon_0 \varepsilon_D \varepsilon_H}{2(\varepsilon_D d_H + \varepsilon_H d_D)\gamma} V^2 \quad (1)$$

Here, θ is the CA of droplet with the external voltage V, θ_0 is the initial CA without applied voltage, ε_0 is the vacuum permittivity, ε_D is the dielectric constant of the dielectric layer, ε_H is the dielectric constant of the hydrophobic layer, γ is the interfacial tension between the droplet and the surrounding fluid, d_D is the thickness of

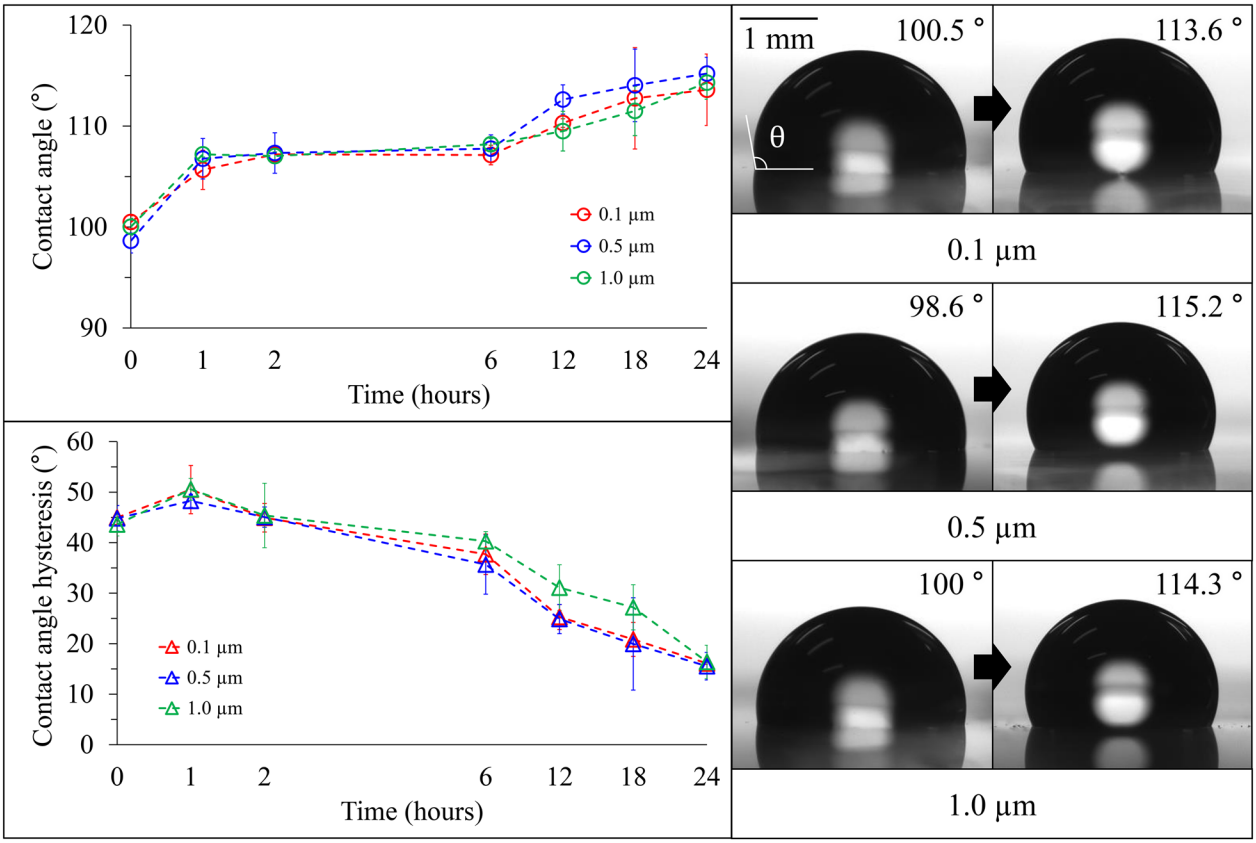

Fig. 7 Graph of the change in contact angle and contact angle hysteresis for heat-treated samples over 24 h

the dielectric layer, and d_H is the thickness of the hydrophobic layer. This equation shows that the thickness of the hydrophobic and dielectric layer affects the change in droplet contact angle with voltage.

Experimental methods

An experimental setup is designed to damage multiple hydrophobic coating samples with falling droplets simultaneously. Figure 3 shows an experimental setup that simulates raindrops to damage hydrophobic coatings. The 3D-printed holder can hold fifteen EWOD samples reliably. The holder is designed to be at an angle of 45° to the ground to allow water to flow away effectively, minimizing damage to the hydrophobic coating from water immersion. Moreover, the holder can be easily mounted in a fixed position on the 10 mm thick acrylic water tank, which not only makes it easy to remove and add samples, but also ensures that the experiment is always performed in the same position. A top water tank is placed 800 mm above the holder, and the water is flowed through a flow regulator, allowing water drops to fall into the center of the sample. Through the flow regulator, 70 microliters of droplets were dispensed at a rate of one drop per second. Then, when the water in the top tank goes below a certain level, the water level regulator activates the water pump to keep the water level constant. This experimental setup allows for the evaluation of different variables in samples simultaneously. And it ensures that the same experimental environment is always maintained, which reduces the gap between damage-recovery experiments and evaluations to examine long-term durability.

The EWOD-structured samples are fabricated for the durability test of hydrophobic coatings. Within every deposition process, test samples are cleaned with acetone and then isopropyl alcohol, followed by rinsing with deionized water. After rinsing, they are first dried using nitrogen and then completely dried in a 120 °C oven. Indium Tin Oxide (ITO) electrodes are deposited on a cleaned 6″ diameter soda lime wafer (0.7 mm thick) using a sputtering process. It is then diced into 25 mm × 25 mm squares. On top of the diced wafers, 1 µm thick SiO_2 is deposited as a dielectric layer using plasma enhanced chemical vapor deposition (PECVD), and the hydrophobic coating, Cytop (CTX-809SP2), is spin coated in 0.1, 0.5, and 1.0 µm thicknesses. The spin-coated Cytop is dried at room temperature for 30 min and then prebaked

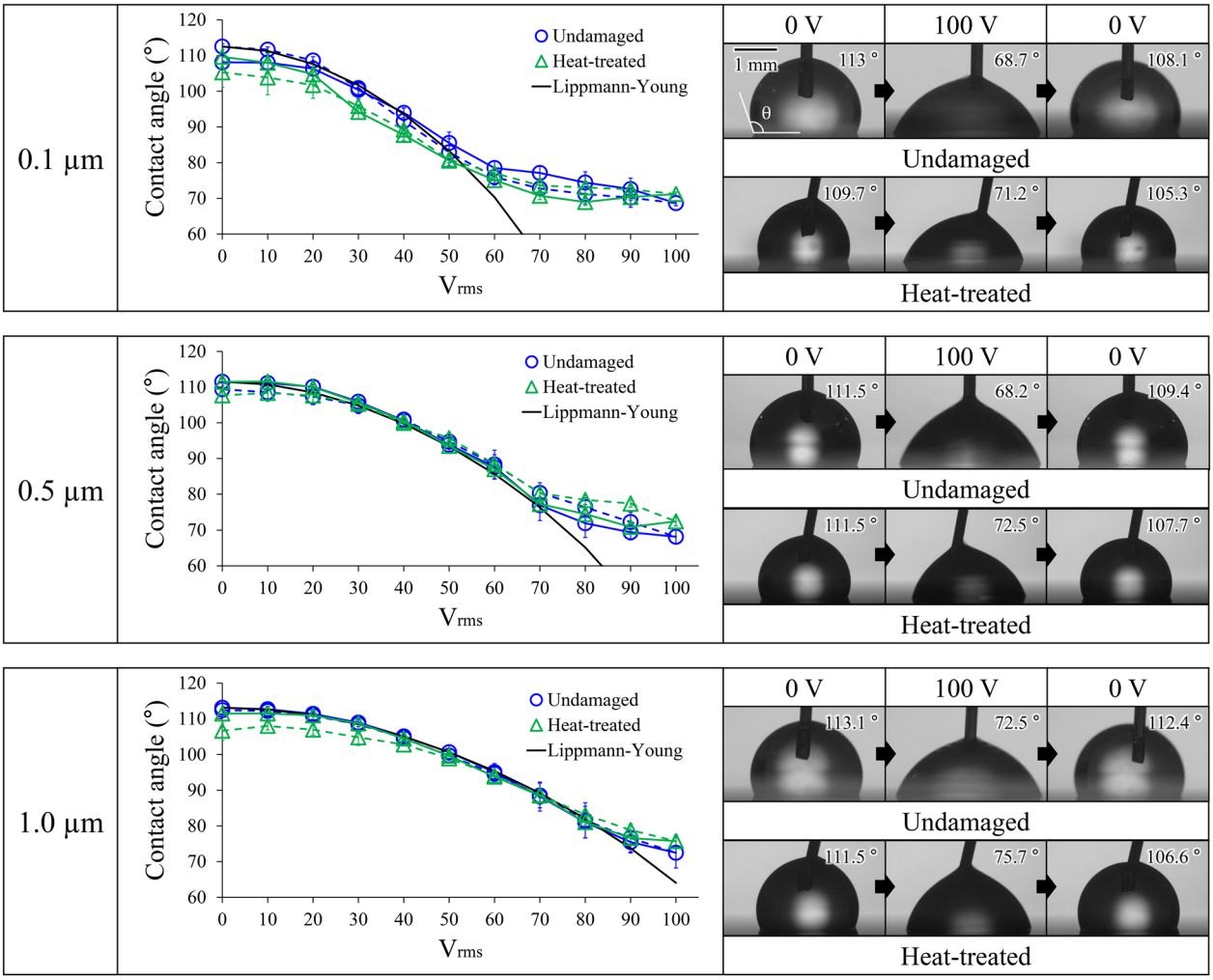

Fig. 8 EWOD hysteresis graph of the undamaged samples and the heat-treated samples after first damage; the solid line is for increasing voltage, and the dashed line is for decreasing voltage

at a temperature of 50 °C for 30 min to remove air bubbles within the Cytop. The Cytop is then heated at 80 °C for 60 min to evaporate the remaining solvent. Finally, a final baking at 250 °C for 60 min is performed to improve the surface adhesion of the Cytop.

The CA and CAH of droplets placed on the sample surface are measured by a contact angle goniometer (Smartdrop, Femtobiomed Inc.) to analyze the hydrophobicity of the experimental samples, as shown in Fig. 4. The CA is measured by averaging the contact angles of the three-phase contact line on both sides of a 5 μL droplet generated on the sample's surface. And the CAH of each sample is measured using the captive method. The volume of a 5 μL droplet is precisely controlled by the syringe. As the syringe then increases the volume and the contact area with the sample of the droplet by dispensing water, the contact angle is measured simultaneously, called the advancing contact angle (θ_{adv}). On the contrary, as the syringe sucks in water, the volume and the contact area with the sample of the droplet decrease, and the contact angle is also measured simultaneously, called the receding contact angle (θ_{rec}). The advancing and receding contact angles are measured through each process, and the CAH of each sample is calculated as the difference between the advancing and receding contact angles.

Results and discussion

Damage

The samples with different thicknesses of hydrophobic coatings are first damaged by falling droplets. Figure 5 shows the change in CA and CAH due to falling droplets for hydrophobic coatings of 0.1, 0.5, and 1.0 μm thickness over 10 days. Regardless of the hydrophobic coating

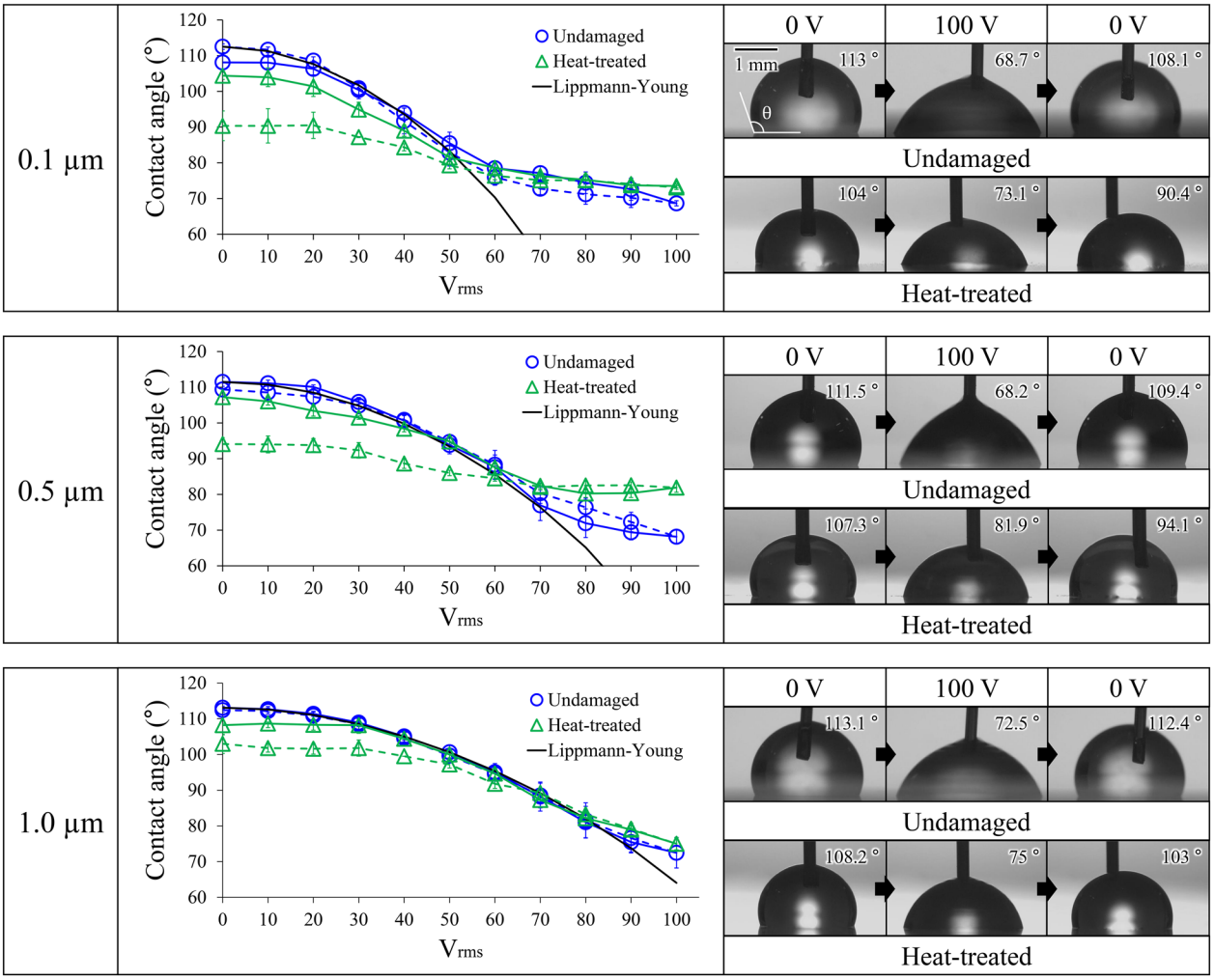

Fig. 9 EWOD hysteresis graph of the undamaged samples and the heat-treated samples after second damage; the solid line is for increasing voltage, and the dashed line is for decreasing voltage

thickness, CA and CAH measure the same before damage, averaging 117° and 13°, respectively. After 10 days of damage, the CA of all samples decrease by about 17° and the CAH increase by about 31°. All samples show a decrease in CA at a rate of 5.7° per day and an increase in CAH at a rate of 10° per day during the initial 3 days. This experiment validate the proposed hydrophobic coating damage method and demonstrate that a 10-day experimental period is sufficient to saturate the damage. It is also experimentally observed that the thickness of the hydrophobic coating does not affect the rate of damage by falling droplets.

The EWOD actuation performance of damaged and undamaged hydrophobic coatings is compared. All the EWOD experiments are performed using a function generator (33210A, Agilent Co.) and amplifier (PZD700, Trek Co.) with a frequency of 1 kHz to measure the change in CA of the droplets by sequentially increasing the voltage from 0 V_{rms} to 100 V_{rms} and decreasing it back to 0 V_{rms}, in 10 V_{rms} increments. The EWOD actuation performance is measured by the ratio of the initial contact angle to the contact angle recovered when the voltage is removed. Figure 6 shows the variation of the experimental measurements of CA and the theoretical value from the Lippmann-Young equation as a function of the voltage of the sample before and after damage. The hydrophobic coating of the undamaged sample is found to have the same trend as the theoretical value under EWOD actuation. In addition, the contact angle of the dewetted droplets after EWOD actuation is recovered by about 98 % on average compared to the initial contact angle, indicating normal EWOD performance. On the other hand, the damaged samples show a significant decrease in droplet wetting and dewetting performance

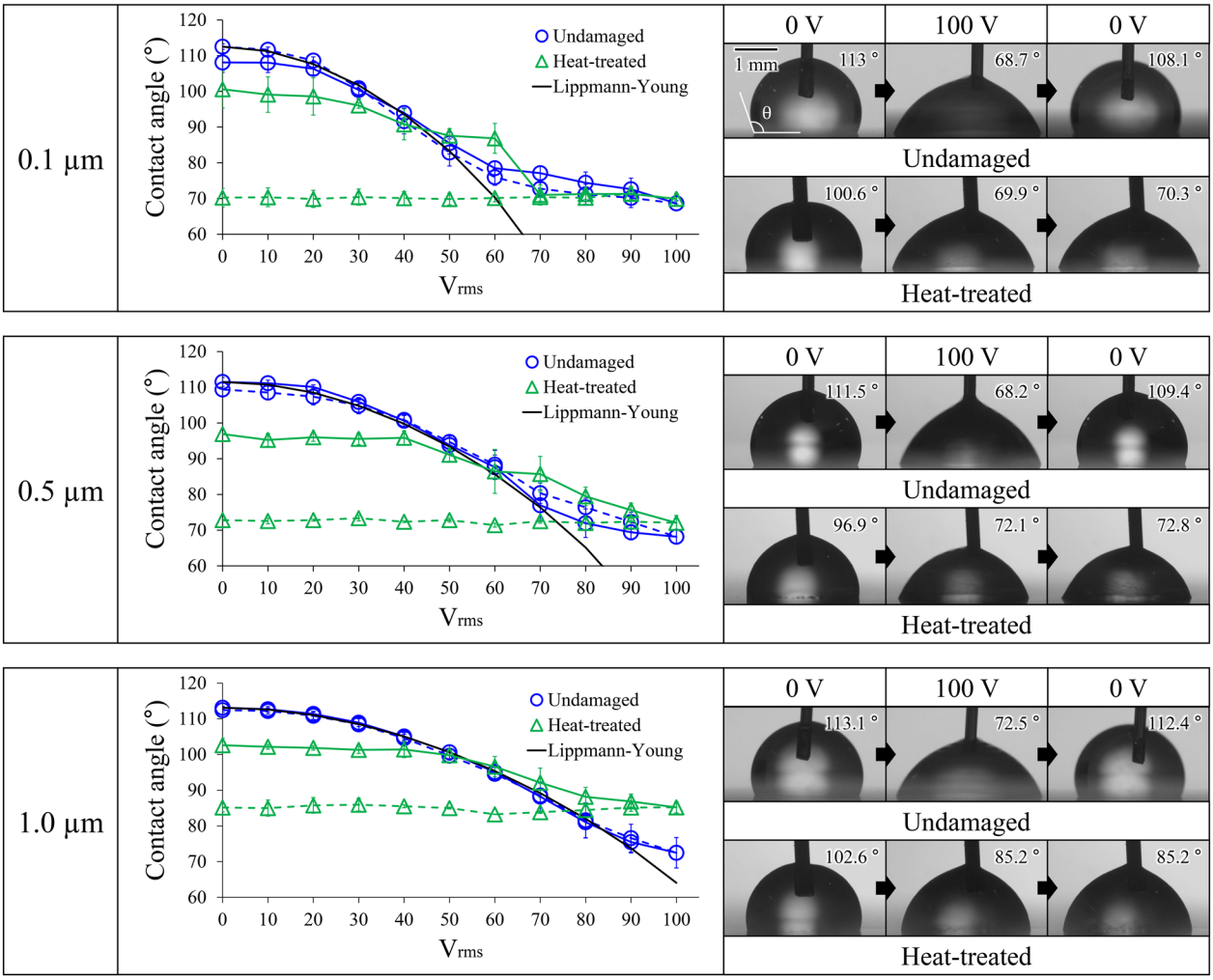

Fig. 10 EWOD hysteresis graph of the undamaged samples and the heat-treated samples after third damage; the solid line is for increasing voltage, and the dashed line is for decreasing voltage

as a function of voltage, regardless of the thickness of the hydrophobic coating.

Recovery

The samples are then heated on a hot plate at 200 °C for 24 h to recover their hydrophobicity damaged by falling droplets, followed by CA and CAH measurements, as shown in Fig. 7. Regardless of the hydrophobic coating thickness, CA and CAH are measured to average 114° and 16° after heating. The experiment shows that CA and CAH recovered about 98 % and 81 %, respectively, compared to before damage. This proves that the damage to the hydrophobic coating caused by the falling droplets can be recovered by annealing at 200 °C. On the other hand, the recovery rate of CA and CAH over 24 h does not differ regardless of hydrophobic coating thickness. This confirms that the thickness of the hydrophobic coating and the rate of hydrophobicity recovery are independent.

Damage-recovery cycle

The EWOD actuation performance is evaluated by repeating the damage-recovery cycle to determine the tendency of the damage-recovery of the hydrophobic coating depending on its thickness. Figure 8 shows the change in CA as a function of voltage for the undamaged sample and the sample that conducted the first damage-recovery cycle. The samples after the first cycle recovered by about 96 % when comparing the CA of the dewetted droplets after the EWOD actuation to the initial CA. Comparing the undamaged sample, where the CA of the dewetting droplet recovers to about 98 % of the initial CA, the sample after the first cycle shows a decrease

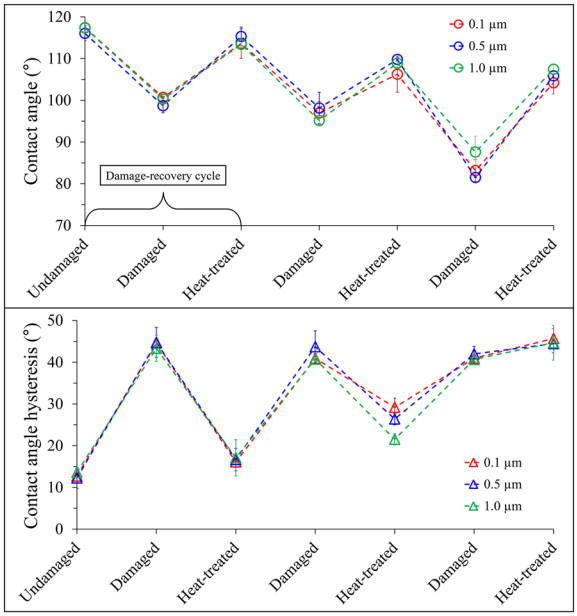

Fig. 11 Graph of the change in contact angle and contact angle hysteresis of samples over repeated damage-recovery cycles

in EWOD performance of about 2 %. This experiment shows that the samples after the first damage-recovery cycle showed no difference in EWOD performance compared to the undamaged samples, and the difference in the degree of damage based on the hydrophobic coating thickness was not observed in the first damage-recovery cycle.

After that, we check the EWOD actuation performance after the second damage-recovery cycle. Figure 9 shows the change in CA as a function of voltage for the undamaged sample and the sample that conducted the second damage-recovery cycle. For the 0.1 μm thick sample after the second cycle, the CA of the dewetted droplet after the EWOD actuation recovered by about 87 % compared to the initial CA before the EWOD actuation, while the 0.5 μm thick sample recovered by 88 %. The 1.0 μm thick sample recovered about 95 %, performing 8 % better than the 0.1 μm thick sample and 7 % better than the 0.5 μm thick sample. This experiment confirms that a thicker hydrophobic coating results in superior long-term durability of EWOD actuation.

Finally, we check the EWOD actuation performance after the third damage-recovery cycle. Figure 10 shows the change in CA as a function of voltage for the undamaged sample and the sample that conducted the third damage-recovery cycle. After the third cycle, no dewetting of the droplets is observed after the EWOD actuation, which means breakdown of the hydrophobic coating, regardless of its thickness. Therefore, it concludes that the damage-recovery of the hydrophobic coating in this falling droplets experiment can not fully perform for three cycles, regardless of the thickness of the hydrophobic coating.

The CA and CAH of water droplets placed on the surface of the hydrophobic coating are measured after each cycle to determine the relationship between the observed EWOD actuation performance and the change in hydrophobicity of the coating, as shown in Fig. 11. Similar to

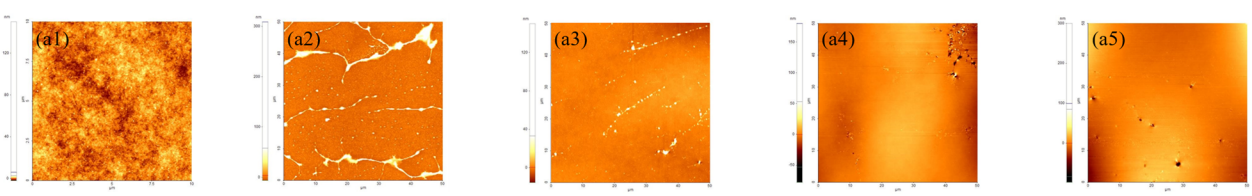

		Roughness	
		Ra (nm)	Rq (nm)
(a1)	Undamaged	0.398	0.513
(a2)	Damaged	6.913	16.207
(a3)	After the first damage-recovery cycle	2.000	5.027
(a4)	After the second damage-recovery cycle	6.037	7.495
(a5)	After the third damage-recovery cycle	8.520	11.387

Fig. 12 Atomic force microscopy (AFM) images of surface changes in the 1.0 μm thickness of CYTOP in each damage-recovery cycle

the results of the previous experiments, the hydrophobicity of the hydrophobic coating in the first cycle shows little difference from the hydrophobicity of the undamaged coating, and in the second cycle, the thicker the hydrophobic coating, the better the hydrophobicity shows. After the third cycle, the CA has recovered 90 % of the initial CA, but the CAH has increased by about 375 % of the initial CAH, which is consistent with the results of the EWOD performance.

The surface morphology of the 1.0 μm samples are analyzed using atomic force microscopy for each cycle. Figure 12 shows the change in surface morphology of the hydrophobic coating and its roughness changes. Ridges appeared on the surface of the damaged coating, represented by white areas, increasing the surface roughness. This is likely caused by the constant impact of falling droplets and exposure to water. Through the reflow which occurs by heating the damaged coating, the white area seen in (a2) is reduced in (a3).

The roughness gradually increased with each repeated damage-recovery cycle. The high roughness of the surface makes it difficult for water droplets to slide easily. Therefore, it is likely to have had a significant impact on the increase in CAH. However, it is difficult to explain the degradation of CA only due to a change in surface morphology. Chemical changes on the surface will also play an important role in CA degradation [30].

Conclusion

This study evaluates the long-term durability of hydrophobic coatings for open-air EWOD devices. Cytop (CTX-809SP2), a fluoropolymer-based hydrophobic coating, was subjected to a continuous damage-recovery cycle, and the EWOD actuation performance was analyzed as a function of hydrophobic coating thickness in each cycle. Regardless of the thickness of the hydrophobic coating, the performance of the EWOD actuation has degraded with each repeated cycle. However, after the second damage-recovery cycle, the thickest 1.0 μm sample showed 8 % and 7 % higher EWOD performance than the other samples, respectively. The second cycle showed that the thickness of the hydrophobic coating affects the hydrophobicity damage caused by falling droplets. Furthermore, after the third damage-recovery cycle, EWOD performance degraded significantly for all samples, experimentally demonstrating the number of recovery limitations of the hydrophobicity of the coating. This study verified the number of recovery limitations of different thicknesses of Cytop through raindrop simulation, which will provide useful information for durability evaluation methods and thickness selection for open-air EWOD devices and for further research on hydrophobic coating durability. Although thicker hydrophobic coatings showed the best durability against falling droplets, it should be noted that the required voltage for EWOD actuation increases with increasing thickness. Therefore, future research should analyze and optimize the correlation between the long-term durability of open-air EWOD devices and the voltage for EWOD actuation. This research is expected to provide a basis for future research and applications of EWOD technology.

Acknowledgements
Not applicable.

Author contributions
YS: conceptualization, figure preparation, experiment design, data analysis, writing—original manuscript; DL: data curation, writing—review & editing; WK: experiment design, data analysis; SKC: conceptualization, supervision, and project administration. All the authors read and approved the final manuscript.

Funding
No funding was received.

Availability of data and materials
Data sharing is not applicable to this article.

Declarations

Competing interests
The authors declare that they have no known competing financial interests or personal relationships that could have appeared to influence the work reported in this paper.

Received: 7 November 2023 Accepted: 20 December 2023
Published online: 08 January 2024

References

1. Sethi SK, Manik G (2018) Recent progress in super hydrophobic/hydrophilic self-cleaning surfaces for various industrial applications: a review. Polym Plast Technol Eng 57:1932–1952. https://doi.org/10.1080/03602559.2018.1447128
2. Trapuzzano M, Crane NB, Guldiken R, Tejada-Martínez A (2020) Wetting metamorphosis of hydrophobic fluoropolymer coatings submerged in water and ultrasonically vibrated. J Coat Technol Res 17:633–642. https://doi.org/10.1007/s11998-019-00250-1
3. Banpurkar AG, Sawane Y, Wadhai SM et al (2017) Spontaneous electrification of fluoropolymer–water interfaces probed by electrowetting. Faraday Discuss 199:29–47. https://doi.org/10.1039/C6FD00245E
4. Chae JB, Kwon JO, Yang JS et al (2014) Optimum thickness of hydrophobic layer for operating voltage reduction in EWOD systems. Sens Actuators A Phys 215:8–16. https://doi.org/10.1016/j.sna.2013.11.001
5. Fillafer C, Ratzinger G, Neumann J et al (2009) An acoustically-driven biochip—impact of flow on the cell-association of targeted drug carriers. Lab Chip 9:2782–2788. https://doi.org/10.1039/B906006E
6. Schneider MF, Guttenberg Z, Schneider SW et al (2008) An acoustically driven microliter flow chamber on a chip (μFCC) for cell–cell and cell–surface interaction studies. Chem Phys Chem 9:641–645. https://doi.org/10.1002/cphc.200700566
7. Ahamed MJ, Gubarenko SI, Ben-Mrad R, Sullivan P (2010) A Piezoactuated droplet-dispensing microfluidic chip. J Microelectromech Syst 19:110–119. https://doi.org/10.1109/JMEMS.2009.2036866
8. Okochi M, Tsuchiya H, Kumazawa F et al (2010) Droplet-based gene expression analysis using a device with magnetic force-based-droplet-handling system. J Biosci Bioeng 109:193–197. https://doi.org/10.1016/j.jbiosc.2009.07.005

9. Chen SH (1999) Thermocapillary migration of a fluid sphere parallel to an insulated plane. Langmuir 15:8618–8626. https://doi.org/10.1021/la990641b
10. Selva B, Miralles V, Cantat I, Jullien M-C (2010) Thermocapillary actuation by optimized resistor pattern: bubbles and droplets displacing, switching and trapping. Lab Chip 10:1835–1840. https://doi.org/10.1039/C001900C
11. Yakhshi-Tafti E, Cho HJ, Kumar R (2010) Droplet actuation on a liquid layer due to thermocapillary motion: shape effect. Appl Phys Lett 96:264101. https://doi.org/10.1063/1.3456391
12. Fair RB (2007) Digital microfluidics: is a true lab-on-a-chip possible? Microfluid Nanofluidics 3:245–281. https://doi.org/10.1007/s10404-007-0161-8
13. Haeberle S, Zengerle R (2007) Microfluidic platforms for lab-on-a-chip applications. Lab Chip 7:1094–1110. https://doi.org/10.1039/B706364B
14. Zeng J, Korsmeyer T (2004) Principles of droplet electrohydrodynamics for lab-on-a-chip. Lab Chip 4:265–277. https://doi.org/10.1039/B403082F
15. Berge B, Peseux J (2000) Variable focal lens controlled by an external voltage: an application of electrowetting. Eur Phys J E 3:159–163. https://doi.org/10.1007/s101890070029
16. Krupenkin T, Yang S, Mach P (2003) Tunable liquid microlens. Appl Phys Lett 82:316–318. https://doi.org/10.1063/1.1536033
17. Kuiper S, Hendriks BHW (2004) Variable-focus liquid lens for miniature cameras. Appl Phys Lett 85:1128–1130. https://doi.org/10.1063/1.1779954
18. Oh SH, Rhee K, Chung SK (2016) Electromagnetically driven liquid lens. Sens Actuators A Phys 240:153–159. https://doi.org/10.1016/j.sna.2016.01.048
19. Lee J, Park Y, Chung SK (2019) Multifunctional liquid lens for variable focus and aperture. Sens Actuators A Phys 287:177–184. https://doi.org/10.1016/j.sna.2019.01.014
20. Lee J, Park Y, Jang D, Chung SK (2021) Switchable liquid shutter operated by electrowetting for security of mobile electronics. Rev Sci Instrum 92:055009. https://doi.org/10.1063/5.0043841
21. Beni G, Tenan MA (1981) Dynamics of electrowetting displays. J Appl Phys 52:6011–6015. https://doi.org/10.1063/1.329822
22. Hayes RA, Feenstra BJ (2003) Video-speed electronic paper based on electrowetting. Nature 425:383–385. https://doi.org/10.1038/nature01988
23. Roques-Carmes T, Hayes RA, Feenstra BJ, Schlangen LJM (2004) Liquid behavior inside a reflective display pixel based on electrowetting. J Appl Phys 95:4389–4396. https://doi.org/10.1063/1.1667595
24. Yong Lee K, Hong J, Chung SK (2017) Smart self-cleaning lens cover for miniature cameras of automobiles. Sens Actuators B Chem 239:754–758. https://doi.org/10.1016/j.snb.2016.08.032
25. Wu H, Mendel N, van den Ende D et al (2020) Energy harvesting from drops impacting onto charged surfaces. Phys Rev Lett 125:78301. https://doi.org/10.1103/PhysRevLett.125.078301
26. Riaud A, Wang C, Zhou J et al (2021) Hydrodynamic constraints on the energy efficiency of droplet electricity generators. Microsyst Nanoeng 7:49. https://doi.org/10.1038/s41378-021-00269-8
27. Tan J, Wang H, Sun M et al (2021) Regulating droplet impact on a solid hydrophobic surface through alternating current electrowetting-on-dielectric. Phys Fluids 33:042101. https://doi.org/10.1063/5.0044823
28. Chen G, Liu X, Li S et al (2018) A droplet energy harvesting and actuation system for self-powered digital microfluidics. Lab Chip 18:1026–1034. https://doi.org/10.1039/C7LC01259D
29. Wijewardhana KR, Shen T-Z, Jayaweera EN et al (2018) Hybrid nanogenerator and enhancement of water–solid contact electrification using triboelectric charge supplier. Nano Energy 52:402–407. https://doi.org/10.1016/j.nanoen.2018.08.016
30. Bonfante G, Maillard M, Chevalliot S et al (2018) Failure mode analysis on thermally aged hydrophobic coatings applied to electro wetting. Thin Solid Films 646:53–60. https://doi.org/10.1016/j.tsf.2017.11.034
31. Koo B, Kim C-J (2013) Evaluation of repeated electrowetting on three different fluoropolymer top coatings. J Micromech Microeng 23:067002. https://doi.org/10.1088/0960-1317/23/6/067002
32. Zeng X, Zhang K, Tao G, et al (2014) Teflon wetting and dewetting on EWOD device for chemiluminescence detector. In: 2014 IEEE 27th International conference on micro electro mechanical systems (MEMS), pp 1047–1050. https://doi.org/10.1109/MEMSYS.2014.6765824
33. Naderi P, Grau G (2022) Organic thin-film transistors with inkjet-printed electrodes on hydrophobic Teflon-AF gate dielectric with reversible surface properties. Org Electron 108:106612. https://doi.org/10.1016/j.orgel.2022.106612
34. Teng P, Tian D, Fu H, Wang S (2020) Recent progress of electrowetting for droplet manipulation: from wetting to superwetting systems. Mater Chem Front 4:140–154. https://doi.org/10.1039/C9QM00458K
35. Chung SK, Rhee K, Cho SK (2010) Bubble actuation by electrowetting-on-dielectric (EWOD) and its applications: a review. Int J Precis Eng Manuf 11:991–1006. https://doi.org/10.1007/s12541-010-0121-1
36. Mugele F, Baret JC (2005) Electrowetting: from basics to applications. J Phys Condensed Matter 17:705. https://doi.org/10.1088/0953-8984/17/28/R01
37. Quilliet C, Berge B (2001) Electrowetting: a recent outbreak. Curr Opin Colloid Interface Sci. 6:34–39. https://doi.org/10.1016/S1359-0294(00)00085-6

Publisher's Note